Advances in Targeted Glioma Therapy with Transferrin-Conjugated Gemcitabine-Loaded PLGA Nanoparticles

Ladi Alik Kumar [1], Gurudutta Pattnaik [1], Bhabani Sankar Satapathy [2 *], Himansu Bhusan Samal [1*]

Abstract

Primary brain tumor Glioma has one of the highest fatality rates among brain cancers. Conventional chemotherapy for glioma often suffers from off-target drug loss and suboptimal drug availability in brain tissue. This study aimed to develop a targeted strategy for brain cancer cells using transferrin-conjugated, gemcitabine-loaded poly(lactic-co-glycolic acid) nanoparticles (Tf-GB-PLGA-NPs). GB-PLGA-NPs were prepared via solvent evaporation and nanoprecipitation, followed by conjugation with transferrin. The formulation was characterized for physicochemical properties, in-vitro release, cytotoxicity, apoptosis (U87MG cell line), and in-vivo pharmacokinetics. Tf-GB-PLGA-NPs exhibited a particle size of 143±6.23 nm, a PDI of 0.213, a zeta potential of -25 mV, and an entrapment efficiency of 77.53±1.43%. These nanoparticles showed a spherical morphology and sustained release of gemcitabine (76.54±4.08%) over 24 hours. Tf-GB-PLGA-NPs demonstrated significantly higher cell inhibition against the U87MG cell line compared to GB-PLGA-NPs and pure gemcitabine ($P<0.05$). Apoptosis in U87MG cells was higher with Tf-GB-PLGA-NPs (61.25%) than with GB-PLGA-NPs (31.61%). Additionally, Tf-GB-PLGA-NPs achieved significantly higher concentrations in the brain than pure gemcitabine and GB-PLGA-NPs, with a 11.16-fold increase in AUC0-t (bioavailability) compared to pure gemcitabine solution and a 2.23-fold increase compared to GB-PLGA-NPs. These findings suggest that Tf-GB-PLGA-NPs could be a potent alternative carrier for delivering gemcitabine to the brain for glioma treatment.

Keywords: Glioma, Transferrin, PLGA nanoparticles, Gemcitabine. U87MG. Apoptosis, Pharmacokinetic

Significance | Glioma's high mortality and treatment challenges necessitate innovative strategies like nanoparticle-based drug delivery, enhancing therapy efficiency and prognosis.

*Correspondence. Bhabani Sankar Satapathy, School of Pharmaceutical Sciences, Siksha 'O' Anusandhan (Deemed to be University), Kalinga Nagar, Bhubaneswar, Odisha
Tel : + 7978485114,
E-mail: bhabanisatapathy@soa.ac.in
Himansu Bhusan Samal, Associate Professor Centurion University of Technology and Management, Odisha, India
E-mail: hbsamal@gmail.com

Editor Md. Shamsuddin Sultan Khan, And accepted by the Editorial Board May 14, 2024 (received for review Mar 27, 2024)

1. Introduction

Glioma exhibits one of the most elevated mortality rates among primary brain tumors, constituting approximately 50%–60% of all instances of such tumors (Seker-Polat F et al., 2002). The typical survival period for individuals suffering from glioma remains approximately fourteen months, and 25% of patients survive more than one year. Only 5% of patients survive more than five years post-diagnosis. Glioma is linked with an unfavorable prognosis and is identified by histological features like angiogenesis and tissue necrosis (Kumar LA et al., 2021, Pavithra et al. 2022, Md Shamsuddin et al. 2019, Md Shamsuddin et al. 2017). The microvasculature within gliomas exhibits heterogeneity, potentially impacting the distribution of chemotherapeutic agents to brain tumors. The primary approach for clinical intervention is surgical removal. However, the distinction between tumor and healthy

Author Affiliation.
[1] Centurion University of Technology and Management, Odisha, India,
[2] School of Pharmaceutical Sciences, Siksha 'O' Anusandhan (Deemed to be University), Kalinga Nagar, Bhubaneswar, Odisha

Please cite this article.
Ladi Alik Kumar, Gurudutta Pattnaik et al. (2024). Advances in Targeted Glioma Therapy with Transferrin-Conjugated Gemcitabine-Loaded PLGA Nanoparticles, Journal of Angiotherapy, 8(5), 1-12, 9634

brain tissue is immensely challenging due to uncontrollable infiltration and non-specific growth patterns. As a result, complete surgical eradication of the tumor is usually unattainable (Hormuth II DA et al., 2022). Further, chemotherapeutic drug delivery to brain tumor cells is significantly restricted by the blood-brain barrier (BBB) (Fathi K et al., 2020). Additionally, chemo-medications frequently impose adverse effects on healthy tissues and cells and aggravate the problem. All these factors collectively contribute to the suboptimal outcomes in glioma treatment.

In this context, using nanoparticles (NPs) made from biodegradable polymers has been investigated to address traditional chemotherapy's conventional drawbacks (Li L, Zhang X, Zhou J, Zhang L, and Tao J, 2022; Muhit et al., 2023; Kashifa et al., 2023). NPs can be designed as passive and active targeting tools to transport drug candidates effectively on tumor sites (Shabani L et al., 2023). Actively targeted NPs offer unique advantages in chemotherapeutic drug delivery. They contribute to the retention of drugs within tumor cells by boosting cellular binding and drug accumulation. Furthermore, such NPs enhance the uptake of drugs by leveraging receptor-mediated endocytosis mechanisms (Ferraris C, Cavalli R, Panciani PP, and Battaglia L, 2020; Ikram, 2023).

Now, with the deepening insights into the physiological processes governing the development and sustenance of gliomas, the integration of molecularly targeted substances into conventional chemotherapy regimens emerges as a promising strategy with favorable outcomes. Simultaneously, the angiogenesis pathway generates a multitude of invasion-inhibiting agents, out of which integrin has been demonstrated to be active participation in enhancing glioma adhesion, migration, and angiogenesis (Luo H et al., 2023). Thus, integrating integrin in designing nano-platforms for targeting could be an exciting strategy for efficiently delivering chemotherapeutic agents to glioma. Because of the active role of transferrin receptor (TfR) expression in many cancer types, including glioma, TfR has become a widely used ligand for endothelial cell targets in NP-based active targeting therapy (Su X et al., 2022).

Tf is a plasma glycoprotein (79.5 kDa) containing practical binding domains for Fe^{3+} ions. Tf plays a significant role in binding and transporting iron throughout the body. TfR, a type II transmembrane receptor protein, is found to be expressed heavily on the surface of endothelial cells in glioma (Wang D, Wang C, Wang L, and Chen Y, 2019). It primarily regulates intercellular iron transport and metabolism. It is postulated that an increase in iron requirements by the cancer cells acts as a key guiding factor in the upregulation of TfR in cancerous cells compared to healthy cells. Thus, drug-loaded NPs with Tf surface modification can precisely target TfR with the formation of ligand-receptor complex and can internalized by the cancer cells through receptor-mediated transcytosis (Tiwari P et al., 2023).

Previous studies have already documented the potential of Tf in improving tumor-specific delivery of anticancer drugs loaded through NPs (Hersom et al., 2016)(Koneru T et al., 2021). A study reported by Ramalho et al. showed that Tf-modified PLGA NPs maintained the anti-glioma activity of the loaded Phyto component and increased the cellular internalization in U87MG glioblastoma cells (Ramalho et al., 2022). Tf-conjugated PLGA-NPs were found to be highly adsorbed and endocytosed by BBB endothelial cells (Chang J et al., 2009). A fluorescence microscopic study confirmed higher internalization of Tf-NPs by the tested cell line compared to unconjugated NPs/free drugs (Cui Y, Xu Q, Chow PK, Wang D and Wang CH, 2013). Cui and its associates developed the Tf- Tf-modified magnetic silica PLGA-NPs of doxorubicin and paclitaxel for targeted delivery in glioma cancer. Tf-modified NPs showed the highest cytotoxicity in U-87 cells concerning those treated with unconjugated NPs/free drug/free Tf (Chang J et al., 2012). Tf-conjugated PLGA-NPs improved the anticancer effectiveness of temozolomide and bortezomib in glioblastoma cells, as reported in another recent study (Ramalho MJ et al., 2023).

Gemcitabine (GB) is an FDA-approved, clinically established chemotherapy medication that functions as a nucleoside analog. The GB is a prodrug. Moreover, it converts into active metabolites by switching nucleic acid building blocks during DNA elongation (Dyawanapelly et al., 2017). The active metabolites of GB inhibit malignant cell growth by interfering with DNA synthesis. It destroys cells synthesizing DNA and prevents them from passing the G1/S phase threshold (Shah MA and Schwartz GK, 2006). In clinical practice, Gemcitabine is widely used to treat bladder, breast, pancreatic, non-small cell lung cancer, etc. However, reports on the active targeting of Gemcitabine through Tf-functionalized Gemcitabine PLGA-NPs in glioblastoma cell lines in vitro/in vivo models are scarce. Based on previous literature and a gap in detail study of Tf-functionalized GB-loaded PLGA-NPs, we have already developed and optimized Gemcitabine-loaded PLGA-NPs (Kumar LA et al., 2024). We successfully developed Tf-functionalized GB-loaded PLGA-NPs (Tf-GB-PLGA-NPs) for glioma cell-specific delivery in the present study. The formulation was characterized for physicochemical parameters, invitro release, in-vitro cell line, internalization, cell apoptosis against human glioblastoma cells (U87MG), and pharmacokinetic study in Wistar albino rats.

2. Materials and Methods

2.1 Experimental

Gemcitabine (GB) was obtained from Cipla laboratories (Goa, India) as a gift sample. Poly (lactic-co-glycolic acid (PLGA 50:50) and Transferrin (apo-transferrin bovine, T1428) were procured from Sigma-Aldrich (Mumbai, India). U87MG cell line was procured from NCC, Pune, India. Polyvinyl alcohol (PVA), acetone, and Tween 80 were gathered from Virat Lab, Mumbai

(India). In addition to the chemicals and reagents used in this experiment, all other materials used in the study were a scientific grade.

2.2. Preparation of gemcitabine-loaded PLGA nanoparticles

A slightly modified solvent evaporation and nanoprecipitation technique prepared GB-PLGA-NPs (Kumar LA, 2024). Initially, the formulation was developed in two steps: emulsification of the organic polymer solution into the aqueous surfactant solution, followed by organic solvent evaporation, led to polymer precipitation and nanoparticle formation. The 200 mg of PLGA and 15 mg of GB were dissolved into acetone (10 ml). The aqueous phase containing PVA (1.5%) and 4 ml of tween 80 was prepared separately. Continuous stirring (15000 rpm) for two hours was used to add the organic phase to the aqueous phase. The formed primary emulsion was ultrasonicated for 5 min at 30 sec intervals (Sonics, Vibra cell, vcx750, New Town, USA). The GB-PLGA-NPs were stood overnight for evaporation of the organic solvent. The GB-PLGA-NPs were stored at 25°C. Details of all the optimization processes are discussed in our previous work (Kumar LA et al., 2024)

2.3 Preparation of Tf-decorated Gemcitabine PLGA nanoparticles

An EDC/NHS activation and grafting procedure was used to conjugate Tf on the surface of GB-PLGA-NPs (Nogueira Librelotto DR et al., 2017). Briefly, at first, 2.1 mL of the GB-PLGA-NPs suspension was incubated with EDC (200 µL, 30 mg/mL) under slight stirring at 25°C and NHS (200 µL, 30 mg/mL) for 3 h to obtain amino-reactive esters from the carboxylic acid terminated polymer. After incubation, the sample was filtered by using a centrifugal ultrafiltration unit (Centrisart® 10 kDa MWCO) followed by centrifugation at 2000 g for 40 min to eliminate excess EDC and NHS and unconjugated GB-PLGA-NPs. The ultrafiltrate was collected, and the volume of the GB-PLGA-NPs suspension was adjusted to 2.1 mL with deionized water. Tf solution (300 µL, 10 mg/mL) was added to the GB-PLGA-NPs suspension and was maintained under slight stirring at 25°C for 2h to complete the Tf conjugation. Finally, the sample was filtered by a centrifugal ultrafiltration unit, and ultra-filtrate (Tf- GB-PLGA-NPs) was collected and stored till further analysis.

2.4 Physicochemical Characterization

2.4.1 Fourier-transformed infrared spectroscopy

Fourier-transformed infrared (FT-IR) spectroscopy was used to study the interactions between the drug and the other components of the formulation (FTIR-8400S Shimadzu, Tokyo, Japan). Pure GB, PLGA, Transferrin, GB-PLGA-NPs, and Tf-GB-PLGA-NPs were placed in the instrument and scanned for 4000 to 400 cm−1 at 25°C. (Rai VK, Mishra N, Yadav KS, and Yadav NP, 2018).

2.4.2 Particle size, Zeta Potential, and PDI

The Zeta Sizer (Nano ZS, Malvern Instruments, U.K.) was employed to assess the mean diameter, size distribution (PDI), and zeta potential of the GB-PLGA-NPs, Tf-GB-PLGA-NPs through dynamic light scattering (DLS) method. The diluted sample (1:10) was filled into a respected cuvette and analyzed at 25°C and 90°C scattering angles, represented in Figure 2.(Kumar LA et al., 2024).

2.4.3 Encapsulation efficiency

The dialysis technique was employed to calculate the encapsulation efficiency. The 6 ml of the GB-PLGA-NPs and Tf-GB-PLGA-NPs suspension were filled into a dialysis bag. The 50 ml of 0.1N NaOH was filled into a beaker and stirred at 75 rpm using a magnetic stirrer. The dialysis bag was submerged into a beaker for 60 min for dialysis. One milliliter of dialysis solution was withdrawn periodically at fixed intervals and was checked in a UV-visible spectrophotometer (Lab India 3200) at 281 nm until there was no finding of the drug in the medium (Kumar LA et al., 2024).

2.4.4 Morphology analysis

The morphology of the GB-PLGA-NPs and Tf-GB-PLGA-NPs was done by Transmission electron microscopy (TEM, Jeol JEM 1400 electron microscope, Japan). Briefly, drops of GB-PLGA-NPs and Tf-GB-PLGA-NPs were mounted on copper grids and stained with aqueous uranyl acetate (2% v/v) in water. Then, it was air-dried, followed by visualization under an electron microscope at an 80 kV accelerating voltage.

In vitro Release of drug

The in vitro drug release profile of GB-PLGA-NPs and Tf-GB-PLGA-NPs was conducted using a dialysis bag in phosphate-buffered saline (PBS, pH 7.4). (R. Nogueira-Librelotto et al.,). The required amount of GB-PLGA-NPs and Tf-GB-PLGA-NPs (5mg of GB) were filled into a dialysis tube (MWCO 100Kda), tied at both ends. The tubes were immersed in 37 °C PBS medium and stirred at 100 rpm. 1 ml of medium was withdrawn at definite intervals, and an equal volume of fresh PBS was added to maintain the same volume. The concentration in the sample was analyzed by UV-visible spectroscopy at 281 nm.

2.5 In vitro anticancer potential analysis

2.5.1 Cytotoxicity study by MTT

Vitro the cytotoxic effect of GB-PLGA-NPs and Tf-GB-PLGA-NPs was investigated using the MTT assay method on the U87Mg glioma cell line (CuiY et al., 2013). U87Mg glioma cells were procured from NCCS, Pune, India. The cell line was cultivated in DMEM (Himedia, India) and accompanied by 10% fetal bovine serum (10% FBS), streptomycin (1%), and glutamine (3Mm) at 37 °C in a humidified CO2 incubator up to 2×106 cells/ml cell density. Then, cells were plated into 96 different well plates (Sigma Aldrich, Mannheim, Germany). The cells plated were inoculated with different concentrations (0.01-100µM) of PLGA-NPs, GB-PLGA-NPs, and Tf-GB-PLGA-NPs formulations and incubated for 72 h in the restricted environment. Then 20 µl of cold trichloroacetic acid was added into plates and incubated for 1h at 4°C. The microplate

spectrophotometer (Model 680, Bio-Rad, Japan) was used to measure the optical density (OD) at 490 nm.

2.5.2 Apoptotic analysis

A fluorescence-activated cell sorter (FACS) instrument (BD Biosciences FACS Aria, Germany) was utilized to conduct an apoptotic study on U87M Glioma cells. The cells were maintained in alpha MEM media supplemented with 10 % FBS and the 1% antibiotic-antimycotic solution in the atmosphere of 5% CO2, 18-20% O2 at 37°C temperature in the CO2 incubator and sub-cultured every two days. The cells were cultured and placed at 2×106 cells/ml density in six-well plates (Sigma, Germany). They were then suspended in fresh medium and incubated for 12 h in a humidified CO2 incubator at 37°C. The cells were treated with blank PLGA-NPs, GB-PLGA-NPs, and Tf-GB-PLGA-NPs and incubated for 24h. At the end of the treatment, harvest the cells directly into 12×75mm polystyrene tubes. Centrifuge the tubes for five minutes at 300 g and 25°C. Carefully decant the supernatant and wash the cells twice with PBS. After decanting the PBS completely, add 5 µl of FITC Annexin V in 100 µl of AnnexinV bindingbuffer. Gently vortex the cells and incubate for 15 minutes at 25°C in the dark. Add 5 µl of PI (Propidium Iodide) and 400 µl of 1X Annexin Binding Buffer to each tube and vortexgently. Analyze the samples by flow cytometry immediately after adding PI and measure the % apoptosis or necrosis in all conditions (Derycke ASL et al., 2004).

2.5.3 Internalization efficiency

The internalization efficiency of blank PLGA-NPs, GB-PLGA-NPs and Tf-GB-PLGA-NPs was determined by confocal microscopy (LSM 880 live cell imaging confocal system, Carl Zeiss, Germany). The cells were incubated with FITC labeled with GB-PLGA-NPs and Tf-GB-PLGA-NPs for 0.5 h. The healthy cells were washed with PBS (pH 7.4) to eliminate the formulation from the cell surface and then inoculated into DMEM (Dulbecco's Modified Eagle Medium) culture media. After that, cells were trypsinized using 0.1% w/v trypsin and incubated for 5 min. The cells were harvested using 1 ml of PBS (pH 7.4) and sonicated for 5 min to get cell lysates. Further, it was centrifuged at 8,000 rpm for 15 min, and the supernatant was collected for fluorescence assay (Gurumukhi VC and Bari SB, 2022).

2.6 Animal

Institutional ethical committee approval of the study protocol was obtained from Jeeva Life Science in Telangana, India. The approved protocol number is CCSEA/IACE/JLS/20/11/059. The albino Wistar rats (130-150g male) were used for the study. The rats were housed in standard normal conditions (22°C, dark/light) and were accessible for food and water.

2.7 Pharmacokinetic study

Eighteen albino rats of either sex (130–150 g) were selected for the pharmacokinetic study. We divided the rats into three groups, each with six rats. Before drug administration, rats were fasted overnight. Group I received pure GB solution (10 mg/kg), Group II rats received GB-PLGA-NPs, and Group III rats received Tf-GB-PLGA-NPs(10 mg/kg in PBS) orally. Rat retro-orbital plexus blood samples were collected at various time intervals (0.5, 1, 2,3, 4, 6, 8, and 12 hours) and stored in heparin tubes. Plasma was separated from blood by centrifugation at 3000 rpm for 15 minutes (Remi centrifugal, India) and stored at -70 °C. Using diethyl ether and cervical dislocation, rats were sacrificed after blood was collected. Extracted brains were then washed with saline solution and stored at -70°C. In order to extract GB, 0.5 ml of plasma and brain homogenized were added to 500 µL of 0.5 M PBS (pH 5.9) and 2 ml of diethyl ether. The organic layer was separated after vortexing and centrifuging for 5 minutes at 3500 rpm. After adding 0.2M HCl (200µL) to the organic layer, the tube was vortexed for 5 minutes, then centrifuged at 3000 rpm for 5 minutes. After the organic layer was detached, the acid residue was dried under a nitrogen stream (HGC-12, Tianjin Hengao Ltd., Tianjin, China). We reconstituted the dried samples in 100 µL of mobile phase and analyzed the GB concentration using the HPLC method described in.

2.8 HPLC conditions

The HPLC technique has been employed to measure the concentration of GB in the blood and brain (LC 10 AD model, Shimadzu, Tokyo, Japan). The HPLC setup included a C18 column (250 × 4.6 mm, 5 µm) with an auto-sampler, UV detector, and isocratic pump. Acetonitrile and phosphate buffer (0.023 M, pH 6.6) were used as mobile phase at a 39:61 v/v with a 1ml/min f flow rate. The 0.1% TEA was added into the mobile phase to decrease tailing. The run time was 10 min. The 20 µl of the sample was injected into a column at 25°C, and detection was done using a detector at 281 nm.

3. Results

3.1 Formulation and Characterization of nanoparticles

The GB-PLGA-NPs and Tf-GB-PLGA-NPs were prepared using solvent evaporation and nanoprecipitation techniques with slight modifications (Kumar LA et al., 2024). The GB-PLGA-NPs were successfully conjugated by a two-step EDC/NHS activation and grafting method and denoted as Tf-GB-PLGA-NPs. Physicochemical parameters and in-vitro and preclinical evaluation characterized the formulation.

3.2 FTIR spectroscopy

FTIR spectroscopy depicted successful conjugation of Tf over the NP surface and the absence of any significant interaction between the drug, excipient, or targeting ligands. FTIR spectra of pure GB showed the peaks at 3344 cm-1 (OH stretching), 1674 cm-1 (C=O stretching), and 1602 cm-1 (C-N stretching coupled with NH bending) which can observe in figure 1. The PLGA showed peaks at OH stretching (3333 cm-1), –CH stretching (2997 cm-1), carbonyl

–C = O stretching (1757-1628 cm-1) and C–O stretching (1237 cm-1) (Fig.1B).GB-PLGA-NPs andTf-GB-PLGA-NPs showed the distinctive bands at 3405–3349 cm-1 (O-H stretching), 1540 cm-1 and 1646 cm-1 (carbonyl C=O stretching) (Fig1C-D). These stretching vibration peaks are also present in the FTIR spectra of pure GB. It indicates no significant physical/chemical interaction between the drug and excipients (Nogueira Librelotto Dr et al.m 2017). Additionally, it was confirmed to prove that the characteristic peaks of Tf in the free Tf solution resulted from amide II (~1540 cm−1), amide I (~1650 cm−1) vibrations, and amine N-H stretching (3300−2500 cm−1) at a lower intensity, which was also observed in the Tf-GB-PLGA-NPs, confirming the presence of Tf molecules on the tailored NPs. In addition, the characteristic bands of PLGA and Tf showed minor shifting in the theTf-GB-PLGA-NPs, suggesting the chemical conjugation of PLGA with Tf molecules, with peaks in free Tf shifting from 1540 to 1539 cm-1 and from 1652 cm-1 to 1648 cm-1 respectively. The characteristic peaks of GB in the spectra of GB-PLGA-NPs and Tf-GB-PLGA-NPs are nearly identical, depicting the absence of any major shifting and justifying the absence of any significant physical/chemical interaction.

3.4 Particle size and zeta potential analysis

The average PS of GB-PLGA-NPs and Tf-GB-PLGA-NPs was analyzed and found to be in the nano range, i.e. 139.23±4.65 nm and 143±6.23 nm, respectively Figure. 2A-B. The PS of Tf-GB-PLGA-NPs was slightly higher than GB-PLGA-NPs, owing to the conjugation of Tf on the surface of NPs. PDI of both formulations GB-PLGA-NPs and Tf-GB-PLGA-NPswas 0.311 and 0.213, respectively, justifying the homogenous distribution of NPs. The Zeta potential is one of the critical parameters to investigate the stability of NPs. The zeta potential of GB-PLGA-NPs and Tf-GB-PLGA-NPs were found to be at -21 mV and -25 mV, respectively Figure. 2C-D. An increase in surface charge could be attributed to the presence of Tf on the GNP surface. Higher zeta potential would be helpful to maintain the stability of the formulation in the suspended state (Rai VK et al., 2018).

3.5 Encapsulation efficiency (EE, %)

EE of GB-PLGA-NPs and Tf-GB-PLGA-NPs were analyzed and found to be 78.3 ±1.65% and77.53±1.43%, respectively. The difference in EE might be due to the dissolution and eventual loss in surface adsorbed drugs over Tf-GB-PLGA-NPs (Cui Y et al., 2013) (Dercyke ASL et al., 2004). Higher encapsulation efficiency of the NPs would be crucial for effective in vivo applicability. Further, it was found that surface modification did not significantly affect the drug-carrying capacity of Tf-GB-PLGA-NPs.

3.6 Morphological analysis

TEM images of GB-PLGA-NPs and Tf-GB-PLGA-NPs were analyzed and depicted in Figure 3A-B. The morphology of GB-PLGA-NPs and Tf-GB-PLGA-NPs showed a smooth surface without any imperfections or aggregation. The TEM image was spherical with a clear core-shell structure, as shown in Figure 3. Modifying Tf over the NP surface might result in a slight increase in the structure, as observed in the TEM image.

3.7 In vitro drug release

In vitro, the release of GB from GB-PLGA-NPs and Tf-GB-PLGA-NPs was analyzed by the dialysis bag, and the results are depicted in Figure 4. The GB release from the GB-PLGA-NPs and Tf-GB-PLGA-NPs was found to be 80.13 ±5.24% and 76.54±4.08%, respectively, in 24 h. Both formulations exhibited sustained release of GB over 24h, shown in Figure 4. Sustained release of drugs from the NPs would be helpful for prolonged therapeutic action with reduced dose-related side effects (Gurumukhi VC and Bari SB, 2022)

3.8 In vitro anticancer effectiveness analysis

3.8.1 In-vitro Cytotoxicity assay

To evaluate the cytotoxic potential of GB-PLGA-NPs and Tf-GB-PLGA-NP concerning free GB, an MTT assay was carried out on U87MG glioma cells. The cell viability (%) of GB-PLGA-NPs, Tf-GB-PLGA-NPs, and pure GB are shown in Figure 5. It was observed that cell inhibition depends upon the concentration of GB. The cell variability of the GB-PLGA-NPs, Tf-GB-PLGA-NPs, and pure GB was 46.31±8.24%, 19.05±5.24%, and 9.04±3.41% respectively. IC50 of Tf-GB-PLGA-NPs was found to be significantly less (81.17μM) than GB-PLGA-NPs (41.13 μM) and pure GB solution (81.17μM). Tf-GB-PLGA-NPs exhibited a significantly higher cell inhibition than GB-PLGA-NPs and pure GB at each concentration due to internalization into the cells, which can be observed in Figure 5.

3.8.2 Internalization efficiency

To assess the synergistic cytotoxicity caused by ligand conjugation, intracellular localization of FITC labeled formulation was assessed in U87MG cells. FACS and confocal microscopy assessed cellular uptake efficiency based on Tf conjugation and incubation time. Figures 6A-C show the results. The internalization efficiency formulation concerning fluorescent intensity was analyzed. The order of fluorescent intensity of NPs in U87MG cells is blank PLGA-NPs < GB-PLGA-NPs <Tf-GB-PLGA-NPs in 0.5 h of incubation. Tf-GB-PLGA-NPs showed a significant ($P<0.05\%$) higher internalization into cells (high density of particles into U87MG cells) than blank PLGA-NPs and GB-PLGA-NPs, which can be observed in Figure 6.

3.8.3 Apoptosis analysis

Flow cytometry analysis further confirmed the cytotoxic potential of GB-PLGA-NPs and Tf-GB-PLGA-NPs on U87MG cells; the result is shown in Figure 7. Both early and late apoptosis cell deaths varied significantly among GB-PLGA-NPs, Tf-GB-PLGA-NPs, and blank PLGA-NPs formulations. The percentage of dead cells (upper right quadrant) after applying blank PLGA-NPs, GB-PLGA-NPsand Tf-GB-PLGA-NPs was 0.52%, 40.29%, and 14.66%,

respectively. The % late apoptosis cells (upper right quadrant) was 0.43% for blank PLGA-NPs, 12.85% for GB-PLGA-NPs and 46.57% for Tf-GB-PLGA-NPs, while the % live cells (Lower left quadrant) of the GB-PLGA-NPs, Tf-GB-PLGA-NPs and blank PLGA-NPs was found to be 98.70%, 28.10% and 24.09% respectively. However, the percent of early apoptotic cells (Lower right) was 0.35% for blank PLGA-NPs, 18.76% for GB-PLGA-NPs, and 14.68% for Tf-GB-PLGA-NPs. The % apoptosis of the cells was found to be 0.78% for blank PLGA-NPs, 31.61% for GB-PLGA-NPs, and 61.25% for Tf-GB-PLGA-NPs. It showed that Tf-GB-PLGA-NPs exhibited significantly higher cell death (less viability) than GB-PLGA-NPs, as seen in Figure 7.

3.9 Pharmacokinetic Study

The pharmacokinetic profile (time Vs. concentration) of pure GB, GB-PLGA-NPs, and Tf-GB-PLGA-NPs in plasma and brain samples were analyzed and depicted graphically in figure 8A-B The Cmax, Tmax, AUC0-t of the pure GB solution in plasma was 76.23±6.43µg/ml, 2h, and 180.5±17.43µg.ml/h, while for the GB-PLGA-NPs and Tf-GB-PLGA-NPs, the Cmax, Tmax, AUC0-t in plasma was found to be 89.23±7.12 µg/ml, 2h, and 523.25±32.73 µg.ml/h. and 92.54±8.65µg/ml, 2h, and 555.5±36.51 µg.ml/h, respectively. The Cmax, Tmax, and AUC0-t of the pure GB solution in the brain sample were observed at 39.34±11.27µg/ml, 2h, and 94.37±16. 65µg.ml/h. The Cmax, Tmax, and AUC0-t of the GB-PLGA-NPs and Tf-GB-PLGA-NPs in the brain were found to be 109.76±7.23 µg/ml, 2h, and 568.75±46.49 µg.ml/h. and 201.26±10.54µg/ml, 3h, and 1053.5±53.32 µg.ml/h, respectively (Table 1). The Tf-GB-PLGA-NPs exhibited significantly higher concentration and AUC0-t in the brain than pure GB and GB-PLGA-NPs. Tf-GB-PLGA-NPs showed 11.16-fold higher AUC0-t (bioavailability) than pure GB solution and 2.23-fold higher bioavailability than GB-PLGA-NPs. Tf-GB-PLGA-NPs exhibited significant improvement in half-life and constant slow elimination rate, indicating sustained sustained drug release e. The MRT of Tf-GB-PLGA-NPs in the brain (7.04 h) was significantly ($P<0.05$) higher than the MRT of GB-PLGA-NPs (5.32h) and pure GB (2.37 h) in Table 1. The Cmax of GB from Tf-GB-PLGA-NPs in the brain is significantly ($P<0.05$) higher than pure GB and GB-PLGA-NPs, revealing that significant brain targeting was achieved with Tf surface modification on PLGA-NPs, which can be observed in Figure 8.

4. Discussion

The recent trend in oncology-based research is the active targeting of conventional anticancer drugs through receptor-mediated endocytosis. The tf receptor is highly expressed by vascular endothelial cells in the brain. Thus, modification of Tf over NP surface could be a potential approach in ameliorating the targeting efficiency of drugs to the brain. The experimental Tf-modified PLGA-based NPs were formulated and evaluated successfully.

FTIR spectroscopy provided an essential clue for the successful conjugation of Tf over PLGA-NPs surface as a specific characteristic peak of Tf appeared in the Tf-modified GB-PLGA-NPs. However, there was no significant physical/chemical interaction between GB and NP components.

The PS of the GB-PLGA-NPs and Tf-GB-PLGA-NPswas were found in the acceptable nanosize range (>200nm) for oral delivery approaching the brain. The PS of Tf-GB-PLGA-NPs is slightly more than GB-PLGA-NPs, indicating Tf is decorated over the NPs. Owing to the cationic nature (positive charge) of amine groups of Tf, the zeta potential of Tf-GB-PLGA-NPs showed a higher than GB-PLGA-NPs. Higher surface charge (positive or negative) on NPs is beneficial to maintaining required formulation stability at a dispersed state. Higher similar surface charges between particles, in fact, cause higher repulsive force among particles, which thus helps to maintain a flocculated suspension stage. The desired PS and zeta potential of Tf-GB-PLGA-NP would be helpful for effective brain delivery (Tanavano L et al., 2013). The morphology of NPs did not affect the coating of Tf, which was found to be spherical in both NPs and distributed homogeneously.

The % EE is an essential factor for NPs, which helps to decide the dose and therapeutic efficacy (Nogueria Librelotto D et al., 2017). A higher EE paves the path for the futuristic large-scale production of NPs, whereas a low EE hampers the industrial and clinical suitability. In our case, the EE of GB-PLGA-NPs and Tf-GB-PLGA-NPshave reasonable EE (~80%), which suggests good formulation characteristics. Further, it noted that surface modification did not affect the drug-carrying capacity in Tf-GB-PLGA-NPs.

The release profile of GB from the GB-PLGA-NPs and Tf-GB-PLGA-NPs was evaluated using the dialysis bag and showed initial burst release, which might be due to the release of adsorbed GB onto the NP's surface. However, overall, the release profile was found to be sustained over an extended period of time. NP polymer matrix or erosion of polymer could be responsible for the extended release of drug molecules (Derycke ASL et al., 2004). Sustained release of the drug over an extended period would favor a decrease in dose and potential toxicity of the drug (Rai VK, Mishra N et al., 2018).

MTT assay showed that both GB-PLGA-NPs and Tf-GB-PLGA-NPs formulation exhibited significantly higher cytotoxicity in U87 MG cells than in the pure GB solution (Rai VK, Mishra N et al., 2018). Tf-GB-PLGA-NPs exhibited the highest activity due to drug-sustained release and effective internalization into cells. The higher inhibition of cells of Tf-GB-PLGA-NPs could be due to more internalization into cells (cellular uptake) than GB-PLGA-NPs .

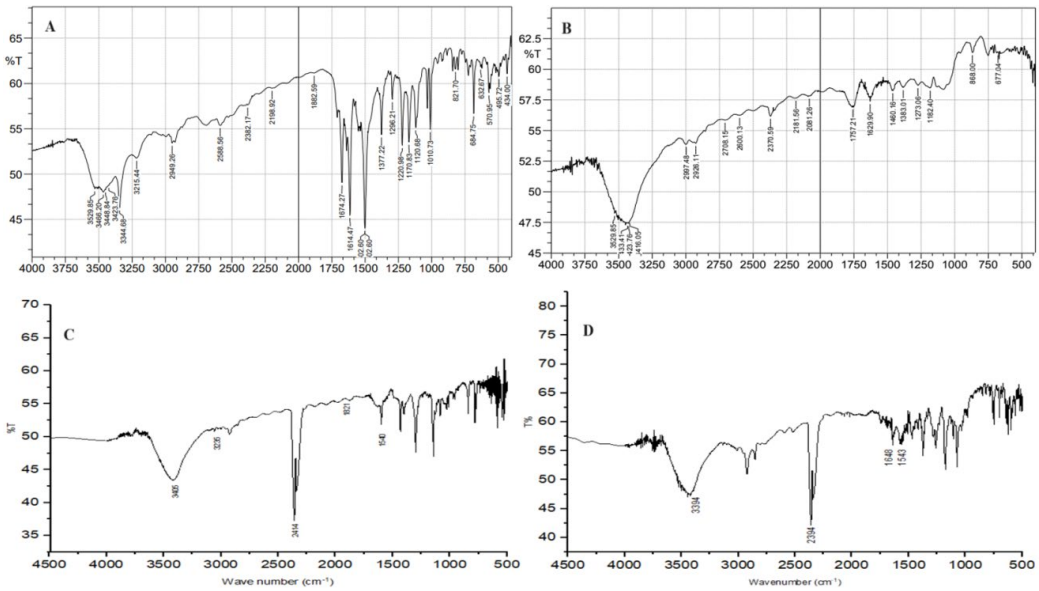

Figure 1. FTIR spectra of (A) pure GB, (B) PLGA, (C) GB-PLGA-NPs, (D) Tf- GB-PLGA-NPs

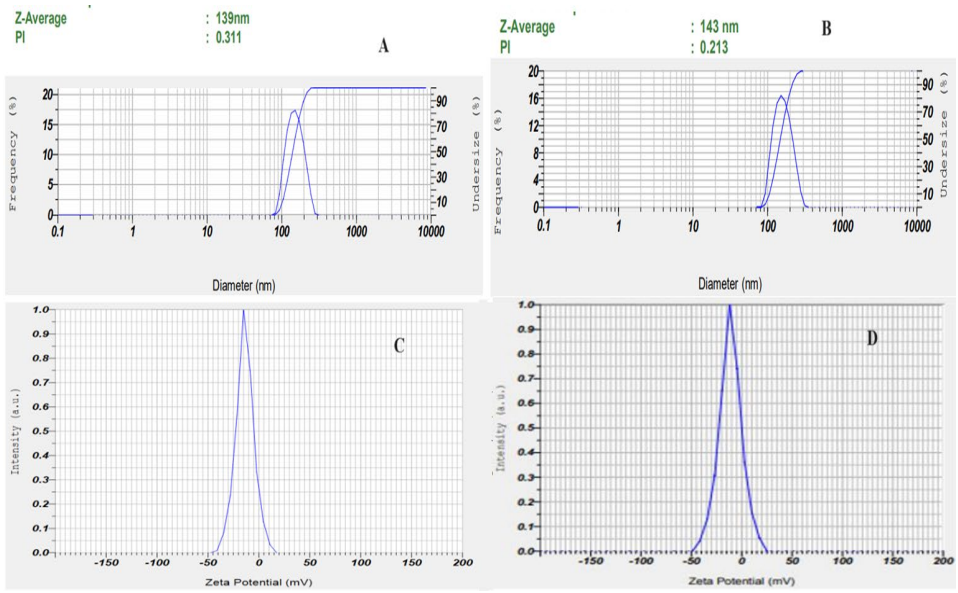

Figure 2. Showing (A) particle size of GB-PLGA-NPs, (B) particle size of Tf-GB-PLGA-NPs, (C) zeta potential of GB-PLGA-NPs (D) zeta potential of Tf-GB-PLGA-NPs

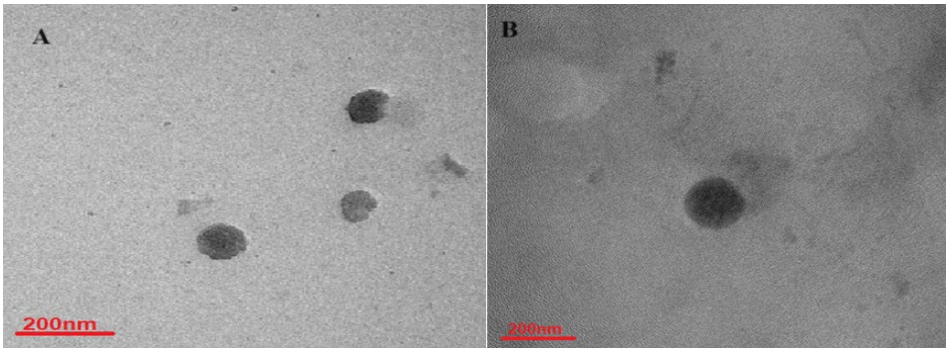

Figure 3. Transmission electron microscopy of (A) GB-PLGA-NPs, (B) Tf- GB-PLGA-NPs

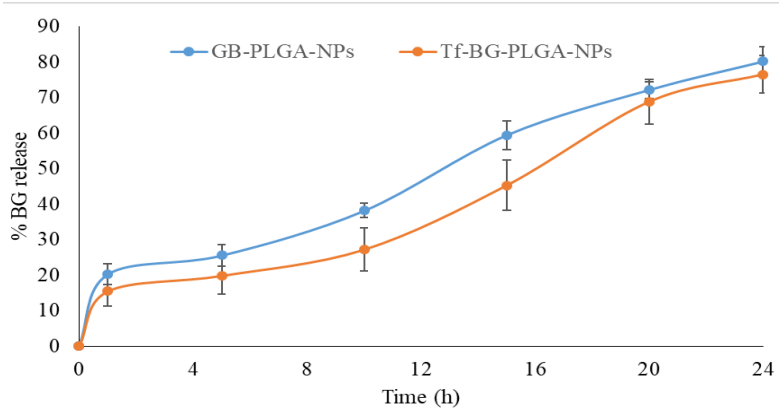

Figure 4. Showing the in-vitro release profile of GB from the GB-PLGA-NPs, and Tf- GB-PLGA-NPs formulations

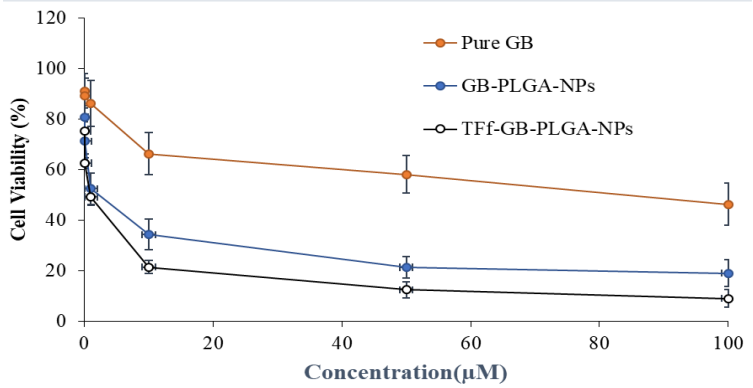

Figure 5. In-vitro cytotoxicity study of pure GB, GB-PLGA-NPs, and Tf- GB-PLGA-NPs against U87MG glioma cells using MTT assay method.

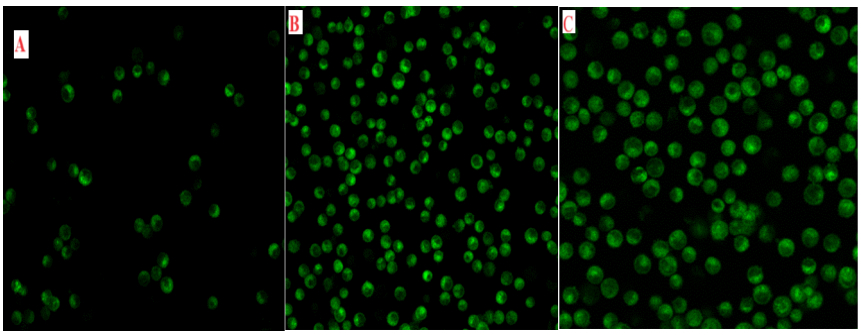

Figure 6. Cellular internalization of labeled formulations against U87MG cells (A) blank PLGA-NPs (B) GB-PLGA-NPs (C) Tf-GB-PLGA-NPs

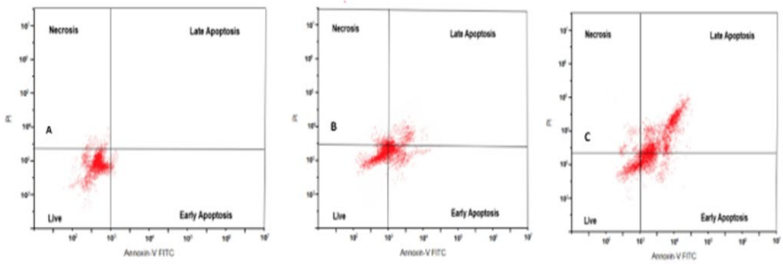

Figure 7. Apoptosis analysis of U87MG cells after application of different formulations (A) blank PLGA-NPs (B) GB-PLGA-NPs (C) Tf-GB-PLGA-NPs

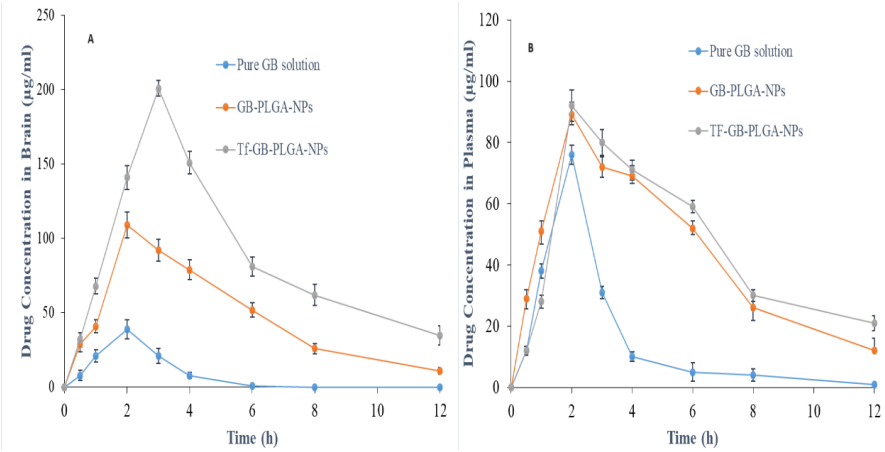

Figure 8. Time-Vs Plasma and Brain concertation of GB (Pharmacokinetic study) from pure GB solution, GB-PLGA-NPs and Tf-GB-PLGA-NPs after oral administration.

Table 1.various pharmacokinetic profile parameters of pure GB solution, GB-PLGA-NPs and Tf-GB-PLGA-NPs after oral delivery in plasma and in brain

Pharmacokinetic parameters	**Plasma**			**Brain**		
	pure GB solution	**GB-PLGA-NPs**	**Tf-GB-PLGA-NPs**	**pure GB solution**	**GB-PLGA-NPs**	**Tf-GB-PLGA-NPs**
Tmax (h)	2	2	2	2	2	3
Cmax (µg/ml)	76.23±6.43	89.23±7.12	92.54±8.65	39.34±11.27	109.76±7.23	201.26±10.54
AUC 0-t (µg.h/ml)	180.5±17.43	523.25±32.73	555.5±36.51	94.37±16.65	568.75±46.49	1053.5±53.32
Half life (h)	1.74	3.39	4.44	0.82	2.93	4.11
Keli (h^{-1})	0.39	0.20	0.15	0.84	0.23	0.17
AUC 0-Inf (µg.h/ml)	183.02±26.24	582.06±29.76	690.08±23.76	94.38±15.72	615.19±20.54	1261.26±29.65
AUMC0-t (µg.h^2/ml)	516.5±27.38	704.43±32.43	2806±37.12	223.79±21.24	2518±31.62	5150±56.92
AUMC 0-inf (µg.h^2/ml)	956a.23±35.26	1510.47±38.54	5283.44±65.23	223.94±30.56	3271.52±43.61	8876.58±56.23

However, Tf-GB-PLGA-NPs may decrease exocytosis than GB-PLGA-NPs and increase cellular uptake (Fazil M et al., 2015). The higher cytotoxic effect of Tf-GB-PLGA-NPs against glioma cells advocates its potential futuristic application in cancer therapy. A similar observation was reported in paclitaxel-PLGA-NPs conjugated Tf (Doijad RC et al., 2008).

Higher cellular uptake suggests the internalization of an adequate quantity of GB-PLGA-NPs and Tf-GB-PLGA-NPs inside the U87MG cells during the pre-fixed incubation period. Owing to higher internalization, the drug could effectively exert its anticancer effect. Further, FITC-labelled Tf-GB-PLGA-NPs showed much higher internalization than GB-PLGA-NPs, confirmed by fluorescence microscopy and suggesting potential targeting efficiency with Tf-conjugation. Fluorescence intensity was highest with FITC labeled Tf-GB-PLGA-NPs due to increased cell membrane permeability and receptor-mediated adhesion of Tf-GB-PLGA-NPs to the cell surface (Zeb A et al., 2022). Modifying the Tf-over NP surface undoubtedly brought higher internalization, favoring its in vivo applicability in the brain tumor model. In addition, FACS was used to assess cellular uptake based on Tf conjugation and incubation time. It have extensively used to quantify the percentage of cells in a sample whose cells are actively undergoing apoptosis through FACS studies. In early apoptosis phases, cells tend to lose membrane asymmetry. In cells staining positive for FITC Annexin V and PI, there is either an end stage of apoptosis, necrosis, or death. As a result, cells that stain negative for both FITC Annexin V and PI are alive and do not show measurable apoptosis. Tf-GB-PLGA-NPs showed sufficiently higher apoptosis than the unconjugated NPs (GB-PLGA-NPs) and blank PLGA-NPs. Tf-GB-PLGA-NPs showed nearly 4-fold higher late apoptotic cell death than the GB-PLGA-NPs (46.5 % Vs. 12.8 %) in 0.5 h incubation. There was a notable difference in the percentage of apoptosis between Tf-GB-PLGA-NPs and GB-PLGA-NPs during both early and late phases. Tf could direct the cells into U87MG cells through receptor-mediated endocytosis (Maghsoudi S et al., 2020).

The results of PK studies suggest a better understanding of conjugate systems over individual drug regimens. For in vivo application and futuristic pre-clinical/clinical suitability, the estimation of PK parameters is an unavoidable tool in targeted/non-targeted nanoformulations. Improved AUC/AUMC of the formulations straightly justifies higher bioavailability. Similarly, higher MRT/T1/2 signifies higher residence time and therapeutic stability of the formulation in an in vivo environment. Tf-GB-PLGA-NPs exhibited significantly higher Cmax, AUC0-t, AUC0-inf, AUMC0-t, AUMC0-inf, and Half-life in the brain than pure GB and GB-PLGA-NPs after oral administration revealing that Tf-GB-PLGA-NPs easily cross the blood-brain barrier (BBB) and reached more drug into the brain than plasma upon Tf decoration. Higher values of AUC and AUMC justify prolonged circulation profile in vivo with higher drug accumulation in brain tissue. The higher half-life and low elimination rate constant in the brain justify targeting the efficiency of Tf-GB-PLGA-NPs. Tf-GB-PLGA-NPs exhibited significantly higher ($P<0.05$) MRT in the brain than GB-PLGA-NPs and pure GB, revealing significant brain targeting. The poor brain uptake of GB is due to its inability to permeate across the BBB and its being a substrate to Pgp (MDR1), efflux transporters present as a blood-brain barrier (Mitra S et al., 2001). The unconjugated and Tf conjugated nanoparticles showed improved brain uptake of the drug. The preferential accumulation of Tf-PLGA-GB-NP across the BBB may result from different events. The abundance of transferrin receptors on BBB could have resulted in receptor-mediated endocytosis (Qian Zm et al., 2002). It can be well documented that surface modification of Tf was able to bring a significant increase in the PK profile compared to non-targeted nano-formulations and free drugs.

5. Conclusion

The work presents an active targeting approach to targeted glioblastoma treatment through developed ligand-modified PLGA-NPs. As a result of surface modification with Transferrin, GB could be successfully loaded into PLGA-NPs and delivered to the brain effectively and sustainably. FTIR study demonstrated the presence of Tf on the NP's surface without any significant physical/chemical interaction. Conjugation of Tfdi does not significantly alter the entrapment efficiency of the drug in NPs. Tf-GB-PLGA-NPs showed significantly higher apoptotic (cell death) in U87MG cells compared to Tf-GB-PLGA-NPs and free GB. Tf-GB-PLGA-NPs also exhibited significantly higher internalization into U87MG cells within 0.5h of incubation. PK study further confirmed higher drug accumulation in the brain tissue. Owing to improved drug availability and higher cytotoxic potential, Tf-GB-PLGA-NPs might be taken for further studies in glioma-bearing xenograft models to pave the way for futuristic clinical applications. In conclusion, the developed formulation strategy could open exciting avenues for advanced glioma treatment.

Author contributions

L.A.K, G.P, B.S.S, H.B.S: Conceptualized the study, developed the methodology, wrote the original draft, and reviewed and edited the manuscript.

Acknowledgment

Authors sincerely acknowledge Centurion University of Technology and Management for constant encouragement and support.

Competing financial interests

The authors have no conflict of interest.

References

Chang J, Jallouli Y, Kroubi M, Yuan XB, Feng W, Kang CS, Pu PY, Betbeder D. (2009). Characterization of endocytosis of transferrin-coated PLGA nanoparticles by the blood–brain barrier. Inte jour. of pharma, 379(2), 285-92.

Chang J, Paillard A, Passirani C, Morille M, Benoit JP, Betbeder D, Garcion E. (2012). Transferrin adsorption onto PLGA nanoparticles governs their interaction with biological systems from blood circulation to brain cancer cells. Pharma. Research, 29, 1495-505.

Cui Y, Xu Q, Chow P.K.-H, Wang D, Wang C.-H. (2013). Transferrin-Conjugated Magnetic Silica PLGA Nanoparticles Loaded with Doxorubicin and Paclitaxel for Brain Glioma Treatment. Biomaterials, 34, 8511–8520.

Cui Y, Xu Q, Chow PK, Wang D, Wang CH. (2013). Transferrin-conjugated magnetic silica PLGA nanoparticles loaded with doxorubicin and paclitaxel for brain glioma treatment. Biomater, 34(33), 8511-20.

Derycke ASL, Kamuhabwa A, Gijsens A, Roskams T, De Vos D, Kasran A, Huwyler J, Missiaen L, De Witte P.A.M. (2004). Transferrin-Conjugated Liposome Targeting of Photosensitizer AlPcS 4 to Rat Bladder Carcinoma Cells. JNCI J. Natl. Cancer Inst, 96, 1620–1630.

Derycke ASL, Kamuhabwa A, Gijsens A, Roskams T, De Vos D, Kasran A, Huwyler J, Missiaen, L.; de Witte, P.A.M. (2004). Transferrin-Conjugated Liposome Targeting of Photosensitizer AlPcS 4 to Rat Bladder Carcinoma Cells. JNCI J. Natl. Cancer Inst, 96, 1620–1630.

Doijad RC, Manvi FV, Godhwani DM, Joseph R, Deshmukh NV. (2008). Formulation and targeting efficiency of Cisplatin engineered solid lipid nanoparticles. Indian J Pharm Sci, 70(2), 203-7.

Dyawanapelly S, Kumar A, Chourasia, MK. (2017). Lessons learned from gemcitabine: Impact of therapeutic carrier systems and gemcitabine's drug conjugates on cancer therapy. Critical Reviews™ in Thera. Drug Carr Syst, 34(1), 63-96.

Fathi Kazerooni, A Bakas ,S Saligheh Rad, H Davatzikos C.(2020). Imaging signatures of glioblastoma molecular characteristics: a radiogenomics review. J. Magn.Reson.Imaging, 52 , 54-69.

Fazil M, Baboota S, Sahni JK, Ameeduzzafar, Ali J. (2015). Bisphosphonates: therapeutics potential and recent advances in drug delivery. Drug Deliv, 22(1), 1-9.

Ferraris C, Cavalli R, Panciani PP, Battaglia L. (2020). Overcoming the blood–brain barrier: successes and challenges in developing nanoparticle-mediated drug delivery systems for the treatment of brain tumours. Int. jour. of nanomed, 30, 2999-3022.

Gurumukhi, V.C.; Bari, S.B. (2022). Quality by Design (QbD)-Based Fabrication of Atazanavir-Loaded Nanostructured Lipid Carriers for Lymph Targeting: Bioavailability Enhancement Using Chylomicron Flow Block Model and Toxicity Studies. Drug Deliv. Transl. Res, 12, 1230–1252.

Hersom M, Helms HC, Pretzer N, Goldeman C, Jensen AI, Severin G, Nielsen MS, Holm R, Brodin B.(2016). Transferrin receptor expression and role in transendothelial transport of transferrin in cultured brain endothelial monolayers. Mole. and Cell. Neuro, 76, 59-67.

Hormuth II DA, Farhat M, Christenson C, Curl B, Quarles CC, Chung C, Yankeelov TE. (2022). Opportunities for improving brain cancer treatment outcomes through imaging-based mathematical modeling of the delivery of radiotherapy and immunotherapy. Adv.Drug Deliv.Rev, 187, 1143-1167

Ikram Ullah Khan. (2023). Synthesis, Characterization and Biomedical Potential of Peptide-Gold Nanoparticle Hydrogels, Biosensors and Nanotheranostics, 2(1), 1-6, 9821

Kashfia Haque, Muhit Rana et al. (2023). Biodegradable Nanoparticles for Sustainable Drug Delivery, Biosensors and Nanotheranostics, 2(1), 1-9, 7334

Koneru T, Mc Cord E, Pawar S, Tatiparti K, Sau S, Iyer AK. (2021). Transferrin: biology and use in receptor-targeted nanotherapy ofgliomas. ACS omega, 6(13), 8727-33.

Kumar LA, Pattnaik G, Satapathy Bhabani S, Mohanty D, Prashanth PA, Dey S, Debata, J. (2024). Preparation and Optimization of Gemcitabine Loaded PLGA Nanoparticle Using Box-Behnken Design for Targeting to Brain: In Vitro Characterization, Cytotoxicity and Apoptosis Study. Curr Nanomat, 9(4), 324-338.

Kumar LA, Pattnaik G, Satapathy BS, Swapna S, Mohanty D.(2021). Targeting to brain tumor: Nanocarrier-based drug delivery platforms, opportunities, and challenges. J. Pharm. Bioallied Sci, 13, 172-177

Li L, Zhang X, Zhou J, Zhang L, Xue J, Tao W.(2022). Non-invasive thermal therapy for tissue engineering and regenerative medicine. Small, 18(36), 2107705-22.

Luo H, Zhang H, Mao J, Cao H, Tao Y, Zhao G, Zhang Z, Zhang N, Liu Z, Zhang, J Luo P. (2023). Exosome-based nanoimmunotherapy targeting TAMs, a promising strategy for glioma. Cell Dea & Dis, 14(4), 235-249.

Maghsoudi S, Taghavi Shahraki B, Rabiee N, Fatahi Y, Dinarvand R, Tavakolizadeh M, Ahmadi S, Rabiee M, Bagherzadeh M, Pourjavadi A, Farhadnejad H, Tahriri M, Webster TJ, Tayebi L. (2020) Burgeoning Polymer Nano Blends for Improved Controlled Drug Release: A Review. Int J Nanomedicine, 15, 4363-4392.

Md Shamsuddin Sultan Khan, Mohammad Adnan Iqbal, Muhammad Asif, Tabinda Azam, Majed Al-Mansoub, Rosenani S. M. A. Haque, Mohammed Khadeer Ahamed Basheer, Aman Shah Abdul Majid, Amin Malik Shah Abdul Majid1, (2019). Anti-GBM potential of Rosmarinic acid and its synthetic derivatives via targeting IL17A mediated angiogenesis pathway. Journal of Angiotherapy, 2(1), 011-011.

Md Shamsuddin Sultan Khan. (2017). Why Interleukin 17A is the most Potential Next Generation Drug Target in Angiogenesis-mediated diseases. Angiotherapy, 1(1), pages 030-032

Mitra S, Gaur U, Ghosh PC, Maitra AN. (2001). Tumour targeted delivery of encapsulated dextran-doxorubicin conjugate using chitosan nanoparticles as carrier. J Control Release, 74(1-3), 317-23.

Muhit Rana, Kashfia Haque et al. (2023). Nanoparticle-Enhanced Drug Delivery Systems for Targeted Cancer Therapy, Biosensors and Nanotheranostics, 2(1), 1-9, 7332

Nogueira-Librelotto D, Codevilla C, Farooqi A, MB Rolim, C. (2017). Transferrin-Conjugated Nanocarriers as Active-Targeted Drug Delivery Platforms for Cancer Therapy. Curr. Pharm. Des, 23, 454–466.

Nogueira-Librelotto DR, Codevilla CF, Farooqi A, Rolim CM. (2017). Transferrin-Conjugated Nanocarriers as Active-Targeted Drug Delivery Platforms for Cancer Therapy. Curr Pharm Des, 23(3), 454-466.

Pavithra Suppiah, Julia Joseph, Rolla Al-Shalabi, Nik Nur Syazni Nik Mohamed kamal, Nozlena Abdul Samad, (2022). Therapeutic Targeting on Death Pathways In Glioblastoma, Journal of Angiotherapy, 6(2), 637-645, 4312

Qian ZM, Li H, Sun H, Ho K. (2002). Targeted drug delivery via the transferrin receptor-mediated endocytosis pathway. Pharmacol Rev, 54(4), 561-87.

Rai VK, Mishra N, Yadav KS, Yadav NP. (2018). Nanoemulsion as pharmaceutical carrier for dermal and transdermal drug delivery: Formulation development, stability issues, basic considerations and applications. J Control Release, 270, 203-225.

Rai VK, Mishra N, Yadav KS, Yadav NP. (2018). Nanoemulsion as pharmaceutical carrier for dermal and transdermal drug delivery: Formulation development, stability issues, basic considerations and applications. J Control Release, 270, 203-225.

Ramalho MJ, Bravo M, Loureiro JA, Lima J, Pereira MC. (2022). Transferrin-modified nanoparticles for targeted delivery of Asiatic acid to glioblastoma cells. Lif Scie, 296, 120435-47.

Ramalho MJ, Torres ID, Loureiro JA, Lima J, Pereira MC. (2023). Transferrin-conjugated plga nanoparticles for co-delivery of Temozolomide and Bortezomib to glioblastoma cells. ACS Applied Nano Mate, 6(15), 14191-203.

Seker-Polat F, Pinarbasi Degirmenci N, Solaroglu I, Bagci-Onder T.(2022). Tumor cell infiltration into the brain in glioblastoma: from mechanisms to clinical perspectives. Cancers, 14, 443.

Shabani L, Abbasi M, Azarnew Z, Amani AM, Vaez A. (2023). Neuro-nanotechnology: diagnostic and therapeutic nano-based strategies in applied neuroscience. BioMed.Engi. OnLine, 22(1), 1-41.

Shah MA, Schwartz GK. (2006). Cyclin dependent kinases as targets for cancer therapy. Update on cancer therapeutics, 1(3), 311-32.

Su X, Zhang X, Liu W, Yang X, An N, Yang F, Sun J, Xing Y, Shang H. (2022). Advances in the application of nanotechnology in reducing cardiotoxicity induced by cancer chemotherapy. InSem. in Can Bio, 86, 929-942.

Tavano L, Muzzalupo R, Mauro L, Pellegrino M, Andò S, Picci N. (2013). Transferrin-Conjugated Pluronic Niosomes as a New Drug Delivery System for Anticancer Therapy. Langmuir, 29, 12638–12646.

Tiwari P, Yadav K, Shukla RP, Gautam S, Marwaha D, Sharma M, Mishra PR.(2023). Surface modification strategies in translocating nano-vesicles across different barriers and the role of bio-vesicles in improving anticancer therapy. Jour. of Contr. Rele, 363, 290-348.

Wang D, Wang C, Wang L, Chen Y. (2019). A comprehensive review in improving delivery of small-molecule chemotherapeutic agents overcoming the blood-brain/brain tumor barriers for glioblastoma treatment. Drug deliv, 26(1), 551-65.

Zeb A, Gul M, Nguyen TTL, Maeng HJ. (2022) Controlled release and targeted drug delivery with poly(lactic-co-glycolic acid) nanoparticles: reviewing two decades of research. J. Pharm. Invest, 52, 683–724.